



Contents lists available at ScienceDirect

Biochemical and Biophysical Research Communications

journal homepage: [www.elsevier.com/locate/ybbrc](http://www.elsevier.com/locate/ybbrc)

# Potent $\gamma$ -secretase inhibitors/modulators interact with amyloid- $\beta$ fibrils but do not inhibit fibrillation: A high-resolution NMR study



Ravichandran Yesuvadian<sup>a,1</sup>, Janarthanan Krishnamoorthy<sup>b,1,2</sup>, Ayyalusamy Ramamoorthy<sup>b,\*</sup>, Anirban Bhunia<sup>c,\*</sup>

<sup>a</sup> Department of Biotechnology, School of Bioengineering, SRM University, Kattankolathur 603203, India

<sup>b</sup> Department of Chemistry and Biophysics, University of Michigan, Ann Arbor, MI 48109-1055, United States

<sup>c</sup> Department of Biophysics, Bose Institute, P-1/12 CIT Scheme VII (M), Kolkata 700054, India

## ARTICLE INFO

### Article history:

Received 24 March 2014

Available online 18 April 2014

### Keywords:

GSM

STD NMR

Sulindac sulfide NMR fibril assay

A $\beta$ 40

## ABSTRACT

Recently,  $\gamma$ -secretase modulators (GSM) have been shown to interact directly with the amyloid precursor protein (APP) and simultaneously inhibit the activity of the Presenilin domain of  $\gamma$ -secretase. A clear understanding of the molecular recognition pathways by which GSM can target both  $\gamma$ -secretase and A $\beta$  precursor protein can lead to the development of more effective inhibitors. To examine whether this direct interaction with APP affects the downstream A $\beta$  fibril formation, we chose to investigate three different molecules in this study: Sulindac sulfide, Semagacestat and E2012 from the class of generation I GSMs,  $\gamma$ -secretase inhibitors (GSI), and generation II GSM molecules, respectively. Firstly, through NMR based ligand titration, we identified that Sulindac sulfide and Semagacestat interact strongly with A $\beta$ 40 monomers, whereas E2012 does not. Secondly, using saturation transfer difference (STD) NMR experiments, we found that all three molecules bind equally well with A $\beta$ 40 fibrils. To determine if these interactions with the monomer/fibril lead to a viable inhibition of the fibrillation process, we designed an NMR based time-dependent assay and accurately distinguished the inhibitors from the non-inhibitors within a short period of 12 h. Based on this pre-seeded fibril assay, we conclude that none of these molecules inhibit the ongoing fibrillation, rather ligands such as Semagacestat and E2012 accelerated the rate of aggregation.

© 2014 Elsevier Inc. All rights reserved.

## 1. Introduction

Alzheimer disease, the most common neurodegenerative disease, is a form of senile dementia characterized by the accumulation of amyloid- $\beta$  (A $\beta$ ) fibril, forming plaques [1] in the brain of the affected patients. Under the physiological condition, the A $\beta$  peptides are generated from amyloid precursor protein (APP) by the sequential cleavage of enzyme complexes namely,  $\alpha$ -secretase,  $\beta$ -secretase and  $\gamma$ -secretase. First,  $\beta$ -secretase cleaves APP in the extracellular domain.  $\gamma$ -secretase then cleaves APP at the  $\epsilon$ -site of the trans-membrane domain resulting in the generation of long peptide fragments such as A $\beta$ 48 and A $\beta$ 49 [2,3]. Further, a stepwise

cleavage of A $\beta$ 48 and A $\beta$ 49 by  $\gamma$ -secretase generate varying lengths of peptide fragments ranging from 37 to 43 amino acid residues. Because of their role in generating toxic A $\beta$  peptides both  $\beta$ -secretase and  $\gamma$ -secretase are considered to be excellent targets for the pharmaceutical drug design. Previous efforts to develop inhibitors for  $\beta$ -secretase have been hindered by a variety of side effects such as interference with the apoptosis pathway and lack of substrate selectivity. Recently,  $\gamma$ -secretase found to be an attractive target for domain specific inhibition/modulation that affects the production of A $\beta$  peptide [3,4]. Several lead molecules have been developed as either  $\gamma$ -secretase inhibitors (GSIs): e.g. Semagacestat, Avagacestat, or  $\gamma$ -secretase modulators (GSMs), e.g. Sulindac sulfide, Flurbiprofen, E2012. The difference between a GSM and GSI lies in the binding site; GSIs are active site inhibitors while GSMs are allosteric modulators. This difference is of functional consequence as  $\gamma$ -secretase has more than 50 other physiological substrates besides APP. Hence  $\gamma$ -secretase inhibitors, in addition to binding with the Presenilin I or II domain, also exhibit non-specific cross inhibitory activity by binding to other domains of  $\gamma$ -secretase, causing adverse reactions [5,6]. To circumvent the non-specificity

\* Corresponding authors. Fax: +1 734 615 3790 (A. Ramamoorthy), +91 33 2355 3886 (A. Bhunia).

E-mail addresses: [ramamoor@umich.edu](mailto:ramamoor@umich.edu) (A. Ramamoorthy), [bhunja@jbose.ac.in](mailto:bhunja@jbose.ac.in) (A. Bhunia).

<sup>1</sup> Both authors contributed equally to this work.

<sup>2</sup> Current address: V ClinBio Pvt Ltd, Central research facility, Sri Ramachandra medical center, Chennai 600116, India.

problem of GSIs, GSMs were developed. GSMs preferentially bind allosterically to the N-terminal fragment of Presenilin, the catalytic subunit of  $\gamma$ -secretase. This selectivity attributes GSMs a higher sensitivity towards the modulation of natural substrate such as APP compared to the other substrates like CD44 and Notch-1 [7].

Certain non-steroidal anti-inflammatory drugs (NSAIDs), such as Sulindac sulfide and Flurbiprofen, apart from inhibiting the COX enzyme also act as potent GSMs. These GSMs have been reported to bind directly to the APP's C-terminal trans-membrane domain (APP TMD) and interfere with the dimerization of APP [4] thereby increasing the accessibility of  $\gamma$ 38 cleavage site of APP compared to the  $\gamma$ 42 cleavage site. This results in the production of the shorter A $\beta$ 38 peptide rather than A $\beta$ 42 [8]. Previous mutation studies have shown that any mutation in the G<sub>29</sub>xxxG<sub>33</sub> motif of APP reduces dimerization drastically and lowers the production of A $\beta$ 42 [8]. GSMs have been shown to bind to this region of APP, diminishing the dimerization and reducing the formation of A $\beta$ 42 [9]. This region corresponds to residues 25–29 of A $\beta$ . Though it is well known that GSMs interact with the G<sub>29</sub>xxxG<sub>33</sub> motif of APP, till date, only limited experimental evidences are available to show how this interaction influence the downstream fibrillation process of A $\beta$ . In this study we are interested in knowing whether first and second generation GSMs, such as Sulindac sulfide, E2012 and GSI, directly interact with A $\beta$ 40 in its monomeric or fibril form to inhibit the fibril formation process.

## 2. Materials and methods

### 2.1. NMR sample preparation

An equivalent of 5 mg of A $\beta$ 40 peptide (China peptides >95% purity) was dissolved in 200  $\mu$ L of HFIP (non-deuterated) and a volume equivalent to 0.1 mg was aliquoted into eppendorf tubes and lyophilized for more than 36 h. A 100 mM stock of Sulindac sulfide (Sigma Aldrich), Semagacestat (Adooq bioscience), E2012 (Adooq bioscience) and Quercetin were prepared in D<sub>6</sub>-DMSO, whereas a 100 mM suspension of  $\beta$ -cyclodextrin was prepared in D<sub>2</sub>O. The A $\beta$ 40 peptide samples used for NMR studies were prepared identically to a final concentration of 80  $\mu$ M by taking the lyophilized peptide equivalent to 0.2 mg and dissolving in 200  $\mu$ L of 2 mM NaOH and allowing it to clarify in a cold room (4 °C) for ~1 h. The clarified sample was vortexed, centrifuged to remove air bubbles and sonicated for 5 min at 4 °C. The NMR sample containing A $\beta$ 40 was in 20 mM of phosphate buffer (pH 7.4), 50 mM of NaCl, and 10% D<sub>2</sub>O. The fibril sample was prepared by dissolving 0.8 mg of lyophilized A $\beta$ 40 peptide in 400  $\mu$ L (2 mM NaOH in D<sub>2</sub>O), with NaCl and sodium phosphate equivalent to 50 and 20 mM concentration, respectively. This sample mixture was incubated at 45 °C in a rotary shaker for more than 48 h. For consistency reasons, the final concentration of the fibril was considered to be the same to that of initial monomer taken. For both fibril seeded kinetics and STD NMR experiments, concentration of fibril was 11.2  $\mu$ M.

### 2.2. NMR experiments

All NMR experiments were performed on a Bruker Avance III 500 MHz spectrometer equipped with a 5 mm SMART probe. In ligand titration based experiments, the conventional 1D with W5 watergate for water suppression was used for the A $\beta$ 40 peptide (80  $\mu$ M) in the presence of the ligand (stock 100 mM) ratios varying from 1:0, 1:0.5, 1:1, 1:2, 1:3 to 1:5. The temperature depended kinetics was performed at different temperatures such 30, 45, 55 and 65 °C by recording 1D NMR spectra over a time period of 12 h, with each data point in the kinetic plot representing an averaged intensity value corresponding to every half hour. The fibril

seeded kinetics were performed identically to the temperature kinetics experiments except that the temperature was set to 40 °C and contained 40  $\mu$ L of 154  $\mu$ M fibril stock incubated previously with 2  $\mu$ L of 100 mM ligand stock for 1 h. The ligands used for the study were Quercetin,  $\beta$ -cyclodextrin, Sulindac sulfide, Semagacestat and E2012. A total of 256 scans were performed for the ligand titrations and 320 scans for temperature kinetic and fibril seeded kinetic experiments. The recycle delay was kept constant at 1 s for all the experiments.

The saturation transfer difference (STD) experiment was recorded for the ligands such as Sulindac sulfide, Semagacestat and E2012 in the presence of fibril at a fibril to ligand ratio of 1:40. The on- and off-resonance saturation was effected by applying a series of selective Gaussian pulse consecutively for a duration of 0.5–5 s at –1 and 40 ppm, respectively. The duration and the inter-pulse delay for saturation pulse were 49 ms and 1 ms, respectively. A total of 960 scans were recorded for STD at 25 °C. A reference spectra with 480 scans was recorded with only the off-resonance saturation and the phase cycle was modified to add the spectra. An inter-scan delay of 1 s was used for both the reference and the STD experiment.

### 2.3. Docking calculations with A $\beta$ fibril

All the docking calculations of three compounds with A $\beta$  fibril were carried out using Autodock. A $\beta$  fibril models (pdb: 2LMO) was taken to studying the binding interaction of small molecules with fibril. Lamarckian genetic algorithm (LGA) was employed as a search engine and LUDI type scoring function was used. Gasteiger–Marsili charges were used for all docking runs and the remaining parameters used were same as that of default settings. The generated binding conformations were grouped into clusters based on the root-mean-squared tolerance of 1 Å for analysis purpose.

## 3. Results

### 3.1. Interaction of GSM/GSI with A $\beta$ monomer

We carried out both qualitative and quantitative analyses of the interaction of a ligand to a protein/peptide by a 1D NMR based ligand titration assay. In this study, the ligands Sulindac sulfide, Semagacestat and E2012 were titrated into A $\beta$ 40 monomers at a peptide to ligand (P:L) molar ratio of 1:0–1:5. As previously reported, the Sulindac sulfide showed a very strong interaction towards the A $\beta$ 40 monomer, even at a ratio of 1:1 [9,10]. This is evident from the significant line-width broadening of the Sulindac resonances appearing close to 7.45 ppm (green trace, Fig. 1A) (Assignment: peaks a, e, f, in Fig. S1). At a P:L ratio of 1:3, Sulindac sulfide induced severe aggregation of the peptide, resulting in a drastic reduction in the peak intensities of the peptide as well as the ligand (blue trace, Fig. 1A). This result is in perfect agreement with the previous study where, the chemical shifts of Sulindac sulfide as well as the aromatic side chain of the peptide were shown to be perturbed during the titration [9,10]. On the other hand, Semagacestat did not interact strongly with the peptide, as evident from its weak perturbation profile for the peptide peaks near 7.78–7.63 ppm (Fig. 1B). Unlike Sulindac sulfide and Semagacestat, E2012 did not interact with monomers of A $\beta$ 40 even at the highest titrated concentration (1:3) used in this study (Fig. 1C).

### 3.2. GSM/GSI binds to A $\beta$ fibrils

Saturation transfer difference NMR is a standard technique to identify the interaction of ligands with biomolecules such as

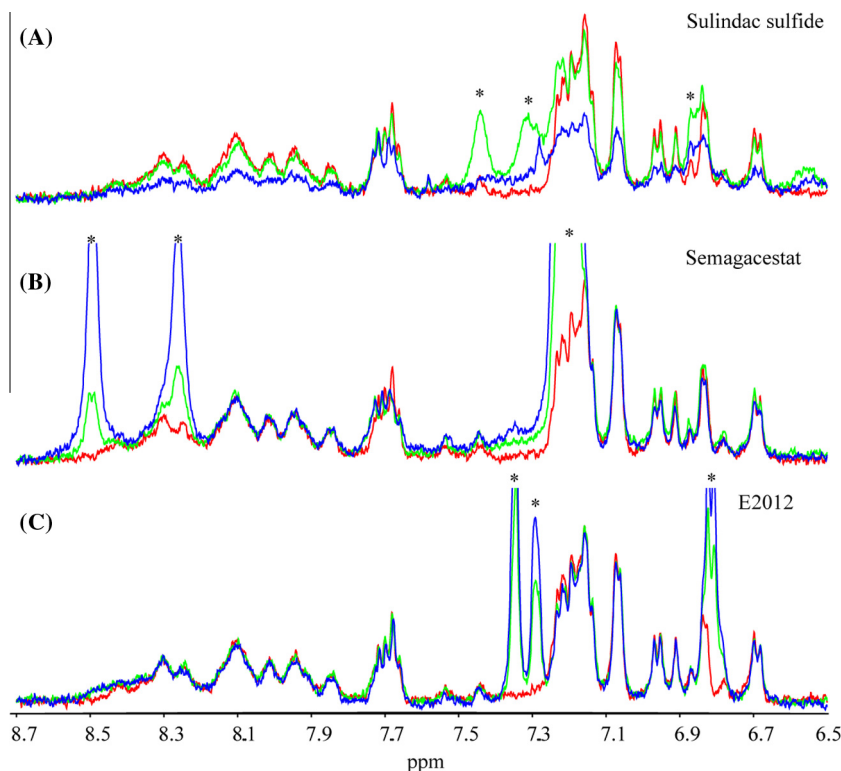


**Fig. 1.** An overlay of the  $^1\text{H}$  titration spectra of A $\beta$ 40 peptide in the presence of Sulindac sulfide (A), Semagacestat (B) and E2012 (C), at the ratio of 1:0 (red), 1:1 (green) and 1:3 (blue). The ligand resonances are indicated as (\*). (For interpretation of the references to color in this figure legend, the reader is referred to the web version of this article.)

protein, virus, lipopolysaccharide (LPS), A $\beta$  fibrils, etc. [11,12]. Recently, STD NMR had been extensively used to specifically identify the specific targets of inhibitors of the A $\beta$  peptide fibrillation process (Fig. S2) [13,14]. We performed STD experiments for three ligands (L) – Sulindac sulfide, Semagacestat and E2012 – in the presence of A $\beta$ 40 fibrils (F) at a molar ratio of 1:40 (F:L). Despite the weak interaction shown by these three ligands towards the monomer, all of them interacted strongly with fibrils (Fig. 2). The group epitope mapping for these molecules were summarized in Fig. 2. The STD effects can be overestimated due to spin–lattice ( $T_1$ ) relaxation effect and hence mislead the group epitope mapping (GEM) of ligand binding to the receptor [11,12]. However, to avoid the  $T_1$  bias, we performed STD experiments at different saturation times, from 0.5 to 5 s, and then obtained the STD amplification factor for each resonance. The amplification factor for a saturation time of 2 s was well below the plateau region to avoid the  $T_1$  bias and hence the overestimation of the STD effects [15–17]. A strong STD effect was determined for the fluorobenzene and the methyl sulphonyl-phenyl ring of the Sulindac sulfide (resonance assignment, Fig. S1). In Semagacestat, the benzazepin ring was found to be in close proximity to the fibril as inferred from the STD spectrum (Fig. S3). Whereas, for E2012, both fluorobenzene and the methoxy-phenyl groups exhibited a strong STD effect relative to the rest of the molecule (Fig. S4).

### 3.3. Fibril seeded kinetics in the presence of GSM/GSI

If fibril seeds are adequately removed, the kinetics of A $\beta$ 40 fibril formation is very slow at 37 °C and spans over a period of 45 days [18]. By adding an aliquot of pre-formed fibril at a ratio of 1:8 (F:P = peptide), we bypassed the slow nucleating lag phase and shifted the fibrillation towards rapid log phase of the sigmoidal curve. We standardized this assay by performing NMR based fibril-seeded kinetic assay for the A $\beta$ 40 monomer, A $\beta$ + $\beta$ -cyclodextrin and A $\beta$ +Quercetin and found the

rate of monomer depletion to be  $3.6 \times 10^{-4} \text{ min}^{-1}$ ,  $2.4 \times 10^{-4} \text{ min}^{-1}$  and  $1.3 \times 10^{-4} \text{ min}^{-1}$ , respectively (Figs. 3, S5). Since, both  $\beta$ -cyclodextrin and Quercetin are well known inhibitors [19,20], the depletion rate of A $\beta$ 40 monomer has decreased considerably relative to the A $\beta$ 40 alone. After validating this assay with control inhibitors, we monitored the effect of GSM/GSI on A $\beta$ 40 fibrillation. The monomer depletion rate in the presence of Sulindac sulfide, Semagacestat and E2012 were,  $3.3 \times 10^{-4} \text{ min}^{-1}$ ,  $6.3 \times 10^{-4} \text{ min}^{-1}$  and  $6.1 \times 10^{-4} \text{ min}^{-1}$ , respectively (Figs. 3, S6). These results clearly indicate that Semagacestat and E2012 accelerated the aggregation process whereas, Sulindac sulfide neither promoted nor inhibited the ongoing fibrillation. Despite these three ligands bind strongly to the fibril as deduced from STD NMR, none of them inhibited the ongoing fibrillation.

### 3.4. Non-fibril seeded kinetics in the presence of GSM/GSI

We also monitored the kinetics of the fibrillation process without addition of any pre-formed fibrils, at increased temperature and ionic strength (Fig. S7). When we compared the intensity loss at 30 °C for the non-fibril seeded kinetics, no discernable changes were evident even at the end of 9 h. Whereas, at higher temperatures such as 45 and 65 °C, significant changes were seen near the chemical shift regions of H $\alpha$  and amide-proton. The loss in the intensity of monomers in non-seeded kinetics at higher temperature was confined only to few resonances compared to the generalized intensity loss observed for the whole peptide in fibril-seeded kinetics.

### 3.5. Docking of GSM/GSI onto the fibril

To obtain further insights into the mode of inhibition, we performed blind docking for all these molecules using a fibril structure (Pdb: 2LMO) and found that Semagacestat and E2012 preferred to dock in the same pocket located at the growing edge (labeled as B) of the fibril (Fig. 4). Whereas, Sulindac sulfide preferred to stick to

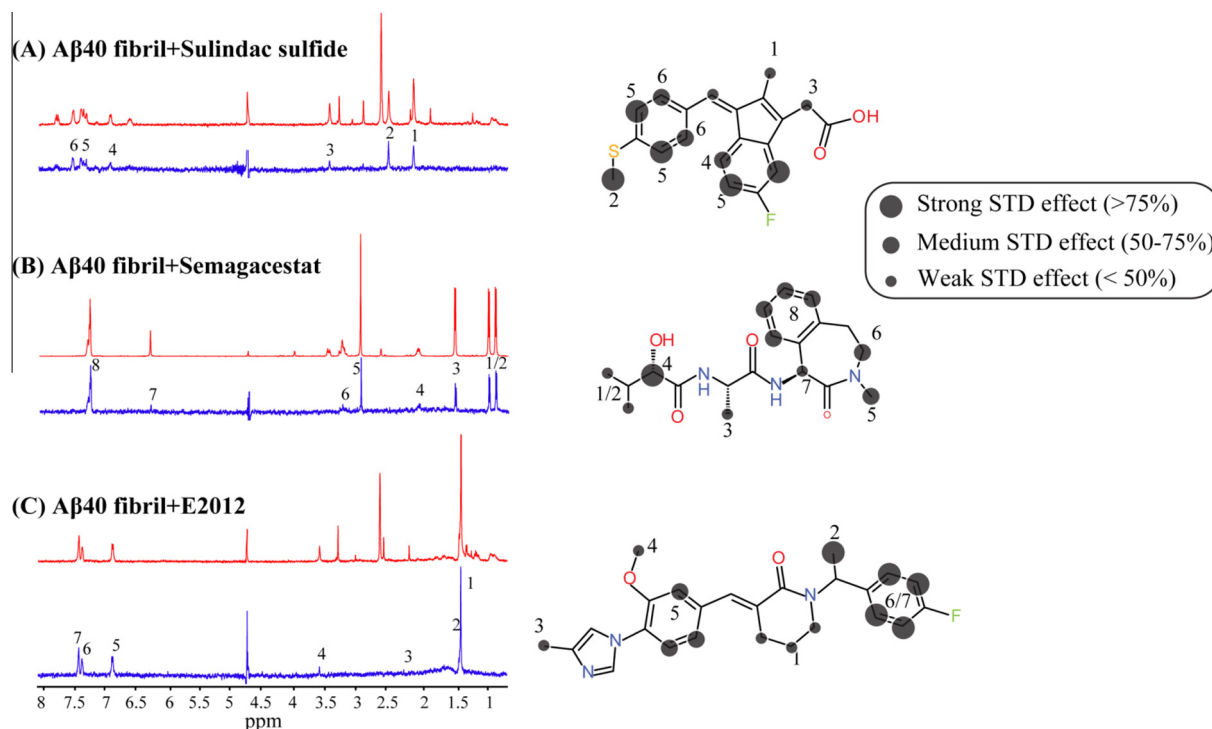


**Fig. 2.** Reference (red) and the corresponding STD spectra (blue) of (A) Sulindac sulfide, (B) Semagacestat and (C) E2012, in the presence of the fibril in a 100% D<sub>2</sub>O. The group epitope mapping of the ligand represented here is based on a scale from strong to weak STD effect corresponding to the area of the circle, respectively. For complete assignment of all of these ligands please refer to Figs. S1, S3, S4. (For interpretation of the references to color in this figure legend, the reader is referred to the web version of this article.)

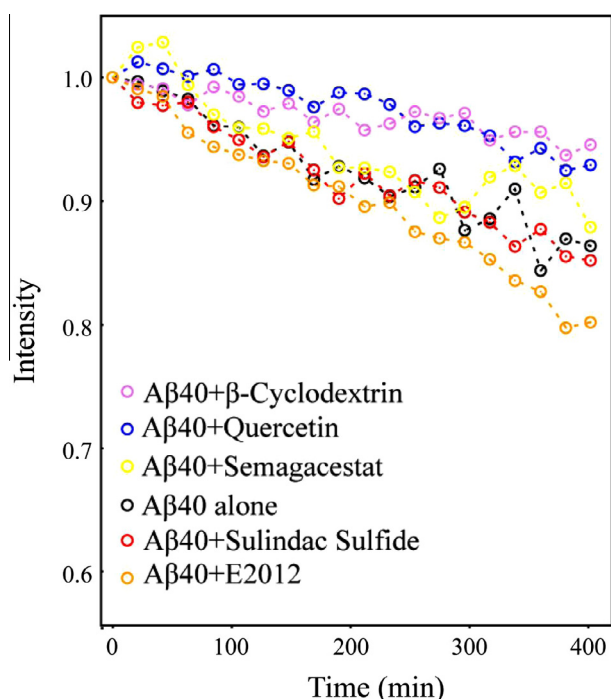


**Fig. 3.** The fibril-seeded monomer depletion assay at 40 °C monitored by the decrease in the intensity in the presence of β-cyclodextrin (blue), Quercetin (violet), Sulindac sulfide (red), Semagacestat (yellow), E2012 (orange). The control monomer depletion assay without any inhibitors is shown in black. In all the cases, the fibril to ligand ratio is 1:80 (fibril = 11.2 μM). (For interpretation of the references to color in this figure legend, the reader is referred to the web version of this article.)

the surface of the filament rather than binding to any of the growing/leading edges. To compare the binding modes of GSMs and GSI with a known inhibitor, we docked Quercetin and found

that it preferred one of the leading edges (labeled A, Fig. 4) placed exactly opposite to that of the Semagacestat and E2012. This binding pocket was close to the central hinge region that connected the N- and C-terminal regions flanked by Ile32, Gly33 and Leu34 on the bottom, and Gly25, Val24, Glu23, Leu22, Ala21, Phe20, Phe19, Val18 and Leu17 on the top. In addition, a strong phenyl ring stacking with Phe19 and Phe20 characterized the binding of Quercetin. The docked orientation of the aromatic ring of Quercetin remained perpendicular to the fibril axis. Contrarily, Semagacestat and E2012, preferred to slide across a groove present near the leading edge and made no contact with the hinge region (Figs. 4 and S8). No phenyl stacking was seen, instead the residues such as Leu18, Val17, Phe19 and Leu34 formed the upper and lower lips of the binding site. At the molecular level, a striking difference seen between Quercetin and Semagacestat/E2012 is that the former molecule is small and rigid, whereas the latter is bulkier and flexible. Infact, these attributes can have a profound effect on the functional aspect of the ligands and dictates whether the ligand remains innocuous or induce/inhibit the fibrillation process. Compared to other GSM/GSI, Sulindac sulfide interacted feebly with Lys16 and Val18 which were present in a shallow pocket exposed to the solvent. It also preferred to stack with Phe20 through a CH- $\pi$  type interaction (Fig. S8). Since its binding pocket is placed significantly away from the growing edges, understandably, the influence of the binding of Sulindac sulfide to the fibril on the fibrillation process is negligible.

#### 4. Discussion

The implication of A $\beta$  amyloid fibril formation in the pathogenesis of Alzheimer disease has been well established [21], but the underlying molecular mechanism of fibril formation from the random coil A $\beta$ 40 monomer to an organized beta sheet fibril through kinetically and thermodynamically rate limiting intermediate



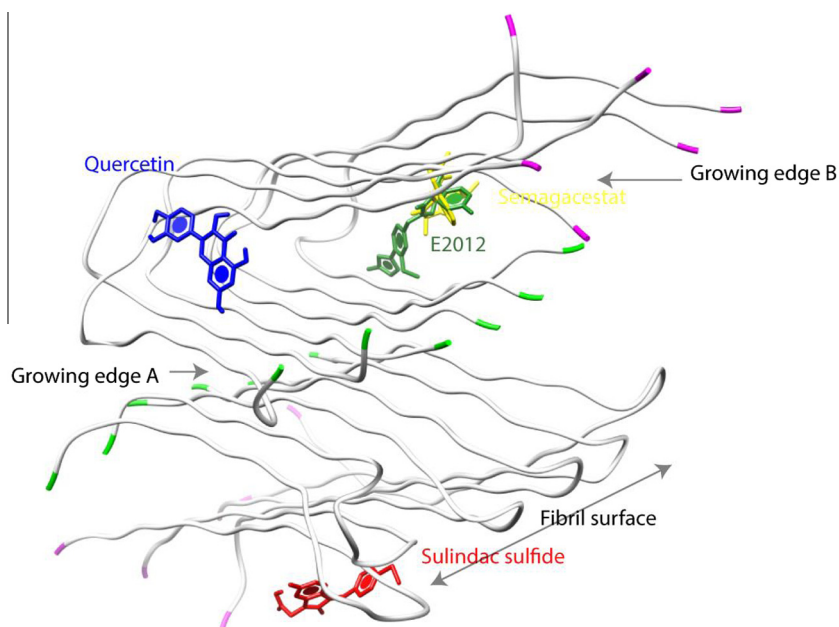


**Fig. 4.** The docked structures of Sulindac sulfide, Semagacestat, E2012 and Quercetin with respect to the A $\beta$ 40 fibril (PDB: 2LMO). The last residue of the N- and C-terminus of the A $\beta$ 40 monomer stacked in the fibril is highlighted in cyan and orange color respectively, to mark out the polarity differences in the growing ends. The aromatic rings of the ligands are represented with a disc to identify the orientation of the rings with respect to the fibril axes. (For interpretation of the references to color in this figure legend, the reader is referred to the web version of this article.)

oligomers, remains obscure even today [22,23]. Recent realization that the formation of ‘intermediate oligomers’ accelerates the fibril formation and the subsequent cell death has lead to the development of new approaches to characterize and monitor these less populated invisible states [24,25]. By default, ThT fluorescence based assay has been commonly used to follow the fibrillation kinetics in the presence or absence of the inhibitors. One major disadvantage of using ThT/other dye in fluorescence assays is that the ThT or fluorescent probes can directly interfere/interact with the ligand, thereby generating artifacts in the assay [26]. On the other hand, in an NMR based kinetics study, we monitor the change in the intensity of the depleting A $\beta$  monomers without addition of any interfering probe molecules. A major drawback in studying the monomer depletion is that its slow kinetics spans over more than 45 days at 37 °C [18].

To tackle this problem, we seeded the A $\beta$  peptide with an aliquot of pre-formed fibril in the ratio of (1:10 of fibril: monomer) and followed the time profile of the monomer using conventional 1D  $^1\text{H}$  NMR at 40 °C. Within a short period of 12 h, we found a decrease in the intensity of monomers. This result is in contrast to another set of experiments where resonance specific intensity variations were observed in non-seeded temperature dependent kinetics. This loss in the intensity for specific resonances in contrast to the generalized intensity loss observed for the whole peptide in fibril-seeded kinetics, is a consequence of the structural exchange and acceleration of amide-solvent exchange at higher temperatures, rather than the monomer depletion. We would like to point out that though the NMR based fibril seeded assay has a direct correlation with the fibril formation, we cannot rule out the possibility that it could be a consequence of the formation of large off-pathway aggregates which remain elusive/invisible to the solution NMR measurements. Hence, further experiments using magic angle spinning solid-state NMR techniques may prove that the depleted monomer is directly related to the on-pathway fibril formation.

We used two positive control inhibitors such as  $\beta$ -cyclodextrin and Quercetin to standardize and validate the NMR based monomer depletion assay. Though it is well established that Quercetin

is a potent inhibitor of A $\beta$ -peptide fibrillation [27,28], the inhibitory mechanism of  $\beta$ -cyclodextrin is not clear. Despite strong evidences from *in vivo* and other biophysical techniques that  $\beta$ -cyclodextrin binds to monomers and prevents the transition from random coil structure to  $\beta$ -sheet [29–31], contrasting results based on DLS measurements suggests that  $\beta$ -cyclodextrin did not prevent/affect the fibrillation of A $\beta$ 40 [32]. The sample of that study contained 2 mM of peptide, 300  $\mu\text{M}$  of ligand and 10 mM HEPES buffer for inducing aggregation. Since the kinetics of the fibrillation process is greatly influenced by the peptide concentration itself, as well as the concentrations of NaCl and phosphate [33], we cannot compare the results of that study with that of our kinetics conducted at a mild condition of 80  $\mu\text{M}$  peptide and 400  $\mu\text{M}$   $\beta$ -cyclodextrin without any HEPES [32]. For  $\beta$ -cyclodextrin and Quercetin, we found that the rate of monomer depletion was decreased by a factor of 1.5 and 2.7 times respectively, in comparison to the non-seeded free monomer depletion.

Based on this assay, we identified that Sulindac sulfide, Semagacestat and E2012 did not prevent the fibrillation process, despite their strong interaction with the fibril. Also the docking results suggest that Quercetin, Semagacestat and E2012 preferred to interact with the growing edges, which are the hot spots for the fibril elongation. Further, the growing edges labelled as A, B (Fig. 4) exhibits an inherent structural polarity, which can possibly affect the functional aspect of the ligand; deciding whether the ligand inhibits/induce or remain innocuous depending on, to which polarity of the growing edge, the binding occurs. To validate these docking results, further experiments are necessary to exactly identify the orientation of the ligand with respect to the fibril axis and relate it to its functional aspects.

## 5. Conclusion

We have developed a simple and efficient NMR based assay to monitor the depletion of the monomer within a short period of time, and demonstrated using control molecules such as Quercetin and  $\beta$ -cyclodextrin that this assay can accurately distinguish the

inhibitors from the non-inhibitors. Adopting this approach, we verified whether the GSMs such as Sulindac sulfide and E2012 had an effect on the downstream A $\beta$ 40 fibrillation process. We found that E2012 enhanced the aggregation kinetics, whereas Sulindac sulfide did not interfere with the fibrillation at all. We also tested Semagacestat, a GSI, which behaved similar to E2012 in its kinetic profile. To explain the mechanistic difference, we docked each ligand onto A $\beta$ 40 fibrils and found that, the ligands that modulate fibrillation process such as E2012 preferred to bind to the leading/growing ends of the fibril (axial surface); whereas Sulindac sulfide, which did not modulate the fibrillation process, interacted primarily with the residues present on the lateral surface of the fibril.

## Acknowledgments

We thank Dr. Jeff Brender, University of Michigan for critical reading of the manuscript. J.K. would like to thank Dr. Mi Hee Lim (Ulsan National Institute of Science and Technology, South Korea) for providing the STD-NMR spectrum of CRP20. The central instrument facility of Bose Institute is greatly acknowledged for 500 MHz NMR instrument facility.

## Appendix A. Supplementary data

Supplementary data associated with this article can be found, in the online version, at <http://dx.doi.org/10.1016/j.bbrc.2014.04.041>.

## References

- [1] S.A. Gravina, L. Ho, C.B. Eckman, K.E. Long, L. Otvos Jr., L.H. Younkin, N. Suzuki, S.G. Younkin, Amyloid beta protein (A beta) in Alzheimer's disease brain. Biochemical and immunocytochemical analysis with antibodies specific for forms ending at A beta 40 or A beta 42, *J. Biol. Chem.* 270 (1995) 7013–7016.
- [2] G. He, W. Luo, P. Li, C. Remmers, W.J. Netzer, J. Hendrick, K. Bettayeb, M. Flajolet, F. Gorelick, L.P. Wennogle, P. Greengard, Gamma-secretase activating protein is a therapeutic target for Alzheimer's disease, *Nature* 467 (2010) 95–98.
- [3] M. Takami, S. Funamoto, Gamma-secretase-dependent proteolysis of transmembrane domain of amyloid precursor protein: successive tri- and tetrapeptide release in amyloid beta-protein production, *Int. J. Alzheimers Dis.* 2012 (2012) 591392.
- [4] A. Ebke, T. Luebbes, A. Fukumori, K. Shirotani, C. Haass, K. Baumann, H. Steiner, Novel gamma-secretase enzyme modulators directly target presenilin protein, *J. Biol. Chem.* 286 (2011) 37181–37186.
- [5] J. Milano, J. McKay, C. Dagenais, L. Foster-Brown, F. Pognan, R. Gadiant, R.T. Jacobs, A. Zacco, B. Greenberg, P.J. Ciaccio, Modulation of notch processing by gamma-secretase inhibitors causes intestinal goblet cell metaplasia and induction of genes known to specify gut secretory lineage differentiation, *Toxicol. Sci.* 82 (2004) 341–358.
- [6] M.S. Wolfe, Inhibition and modulation of gamma-secretase for Alzheimer's disease, *Neurotherapeutics* 5 (2008) 391–398.
- [7] S.A. Sagi, C.B. Lessard, K.D. Winden, H. Maruyama, J.C. Koo, S. Weggen, T.L. Kukar, T.E. Golde, E.H. Koo, Substrate sequence influences gamma-secretase modulator activity, role of the transmembrane domain of the amyloid precursor protein, *J. Biol. Chem.* 286 (2011) 39794–39803.
- [8] B. Bulic, J. Ness, S. Hahn, A. Rennhack, T. Jumpertz, S. Weggen, Chemical biology, molecular mechanism and clinical perspective of gamma-secretase modulators in Alzheimer's disease, *Curr. Neuropharmacol.* 9 (2011) 598–622.
- [9] L. Richter, L.M. Munter, J. Ness, P.W. Hildebrand, M. Dasari, S. Unterreitmeier, B. Bulic, M. Beyersmann, R. Gust, B. Reif, S. Weggen, D. Langosch, G. Multhaup, Amyloid beta 42 peptide (Abeta42)-lowering compounds directly bind to Abeta and interfere with amyloid precursor protein (APP) transmembrane dimerization, *Proc. Natl. Acad. Sci. U.S.A.* 107 (2010) 14597–14602.
- [10] P.J. Barrett, C.R. Sanders, S.A. Kaufman, K. Michelsen, J.B. Jordan, NSAID-based gamma-secretase modulators do not bind to the amyloid-beta polypeptide, *Biochemistry* 50 (2011) 10328–10342.
- [11] A. Bhunia, S. Bhattacharjya, S. Chatterjee, Applications of saturation transfer difference NMR in biological systems, *Drug Discov. Today* 17 (2012) 505–513.
- [12] A. Bhunia, S. Bhattacharjya, Mapping residue-specific contacts of polymyxin B with lipopolysaccharide by saturation transfer difference NMR: insights into outer-membrane disruption and endotoxin neutralization, *Biopolymers* 96 (2011) 273–287.
- [13] J. Milojevic, A. Raditsis, G. Melacini, Human serum albumin inhibits Abeta fibrillization through a "monomer-competitor" mechanism, *Biophys. J.* 97 (2009) 2585–2594.
- [14] S. Lee, X. Zheng, J. Krishnamoorthy, M.G. Savelieff, H.M. Park, J.R. Brender, J.H. Kim, J.S. Derrick, A. Kochi, H.J. Lee, C. Kim, A. Ramamoorthy, M.T. Bowers, M.H. Lim, Rational design of a structural framework with potential use to develop chemical reagents that target and modulate multiple facets of Alzheimer's disease, *J. Am. Chem. Soc.* 136 (2014) 299–310.
- [15] C. Rademacher, N.R. Krishna, M. Palcic, F. Parra, T. Peters, NMR experiments reveal the molecular basis of receptor recognition by a calicivirus, *J. Am. Chem. Soc.* 130 (2008) 3669–3675.
- [16] J. Angulo, P.M. Enriquez-Navas, P.M. Nieto, Ligand-receptor binding affinities from saturation transfer difference (STD) NMR spectroscopy: the binding isotherm of STD initial growth rates, *Chemistry* 16 (2010) 7803–7812.
- [17] M. Mayer, T.L. James, NMR-based characterization of phenothiazines as a RNA binding scaffold, *J. Am. Chem. Soc.* 126 (2004) 4453–4460.
- [18] Y. Suzuki, J.R. Brender, M.T. Soper, J. Krishnamoorthy, Y. Zhou, B.T. Ruotolo, N.A. Kotov, A. Ramamoorthy, E.N. Marsh, Resolution of oligomeric species during the aggregation of Abeta1–40 using (19)F NMR, *Biochemistry* 52 (2013) 1903–1912.
- [19] C. Airolidi, E. Sironi, C. Dias, F. Marcelo, A. Martins, A.P. Rauter, F. Nicotra, J. Jimenez-Barbero, Natural compounds against Alzheimer's disease: molecular recognition of Abeta1–42 peptide by *Salvia sclareoides* extract and its major component, rosmarinic acid, as investigated by NMR, *Chem. Asian J.* 8 (2013) 596–602.
- [20] L.P. Jameson, N.W. Smith, S.V. Dzyuba, Dye-binding assays for evaluation of the effects of small molecule inhibitors on amyloid (Abeta) self-assembly, *ACS Chem. Neurosci.* 3 (2012) 807–819.
- [21] J. Hardy, D. Allosp, Amyloid deposition as the central event in the etiology of Alzheimer's disease, *Trends Pharmacol. Sci.* 12 (1991) 383–388.
- [22] Iryna Benilova, Eric Karran, B.D. Strooper, The toxic A $\beta$  oligomer and Alzheimer's disease: an emperor in need of clothes, *Nat. Neurosci.* 15 (2012) 1–9.
- [23] Minako Hoshi, Michio Sato, Shinichiro Matsumoto, Akihiko Noguchi, Kaori Yasutake, Natsuko Yoshida, K. Sato, Spherical aggregates of  $\beta$ -amyloid (amylospheroid) show high neurotoxicity and activate tau protein kinase I/ glycogen synthase kinase-3 $\beta$ , *Proc. Natl. Acad. Sci. U.S.A.* 100 (2003) 6370–6375.
- [24] L.N. Zhao, H. Long, Y. Mu, L.Y. Chew, The toxicity of amyloid beta oligomers, *Int. J. Mol. Sci.* 13 (2012) 7303–7327.
- [25] Karine Berthelot, Christophe Cullin, S. Lecomte, What does make an amyloid toxic: morphology, structure or interaction with membrane?, *Biochimie* (2012) 1–8.
- [26] S.A. Hudson, H. Ecroyd, T.W. Kee, J.A. Carver, The thioflavin T fluorescence assay for amyloid fibril detection can be biased by the presence of exogenous compounds, *FEBS J.* 276 (2009) 5960–5972.
- [27] K. Ono, Y. Yoshiike, A. Takashima, K. Hasegawa, H. Naiki, M. Yamada, Potent anti-amyloidogenic and fibril-destabilizing effects of polyphenols in vitro: implications for the prevention and therapeutics of Alzheimer's disease, *J. Neurochem.* 87 (2003) 172–181.
- [28] Y. Porat, A. Abramowitz, E. Gazit, Inhibition of amyloid fibril formation by polyphenols: structural similarity and aromatic interactions as a common inhibition mechanism, *Chem. Biol. Drug Des.* 67 (2006) 27–37.
- [29] P. Camilleri, N.J. Haskins, D.R. Howlett, Beta-cyclodextrin interacts with the Alzheimer amyloid beta-A4 peptide, *FEBS Lett.* 341 (1994) 256–258.
- [30] J. Danielsson, J. Jarvet, P. Damberg, A. Graslund, Two-site binding of beta-cyclodextrin to the Alzheimer Abeta(1–40) peptide measured with combined PFG-NMR diffusion and induced chemical shifts, *Biochemistry* 43 (2004) 6261–6269.
- [31] X.R. Qin, H. Abe, H. Nakanishi, NMR and CD studies on the interaction of Alzheimer beta-amyloid peptide (12–28) with beta-cyclodextrin, *Biochem. Biophys. Res. Commun.* 297 (2002) 1011–1015.
- [32] M. Necula, R. Kaye, S. Milton, C.G. Glabe, Small molecule inhibitors of aggregation indicate that amyloid beta oligomerization and fibrillization pathways are independent and distinct, *J. Biol. Chem.* 282 (2007) 10311–10324.
- [33] S. Narayanan, B. Reif, Characterization of chemical exchange between soluble and aggregated states of beta-amyloid by solution-state NMR upon variation of salt conditions, *Biochemistry* 44 (2005) 1444–1452.